CPC(HEP & NP), 2010, **34**(10): 1628–1631 **Chinese Physics C** Vol. 34, No. 10, Oct., 2010

An electrostatic deflector for a fusion reaction *†

ZHANG Huan-Qiao(张焕乔) LIN Cheng-Jian(林承键) YANG Feng(杨峰) JIA Hui-Ming(贾会明)1) ZHOU Ping(周平) AN Guang-Peng(安广朋) ZHANG Chun-Lei(张春雷) XU Xin-Xing(徐新星)

China Institute of Atomic Energy, Beijing 102413, China

Abstract An electrostatic deflector for separating the fusion evaporation residues from the beam-like products in heavy ion reactions was installed. The evaporation residue separation and identification with the electrostatic deflector setup was tested with the reaction ^{32}S+^{96}Zr at several energies. The fusion evaporation residues and the beam-like particles were well separated after the electrical separation and the experimental fusion cross section obtained from the angular distribution is in good agreement with the calculated value well above the Coulomb barrier. This confirms the reliability of the setup.

Key words electrical rigidity, fusion evaporation residues, beam-like products, angular distribution

PACS 29.30.Ep, 25.70.Jj, 25.70.Gh

1 Introduction

The fusion reactions between heavy ions below the Coulomb barrier have been the subject of extensive experimental and theoretical efforts in recent decades. Due to the rich, interesting phenomena unresolved, such as sub-barrier fusion enhancement due to the coupling between the elastic channel and intrinsic degrees of freedom of the target and projectile, and the neutron transfers between the participants compared with the one-dimensional barrier penetration calculation [1], breakup effects of the weakly bound projectiles and the radioactive nuclei on the fusion reactions at near barrier energies [2], neutron-rich effects on the formation of super-heavy elements, especially with the development of the radioactive beams available [1, 3–5], and the fusion hindrance at extremely low energies and the relevant influences on the astrophysics recently found [6], people still point to this field.

However, the experimental identification of fusion evaporation residues (ER) for non-fissile systems is complicated by the fact that they are strongly forward focused into a cone of a few degrees around the beam direction. The background due to the beam-like products resulting from Rutherford scattering in the target and from slit scattering within that angular range demands that the ER be separated physically from the beam-like particles before they reach the detectors. Up to now, a combination of electric and magnetic fields, electromagnetic fields and/or electrostatic fields methods have been used to solve the problem. The electrostatic deflector, which is a simple and cheap device using the electrostatic fields only, can be employed to measure the ER cross sections [7–9]. The ongoing interest in the fusion process mentioned above has led to the building and testing of the electrostatic deflector system. The construction and the experimental results of its performance are reported in this paper.

2 The electrostatic deflector

The fused nuclei, which are concentrated within a few degrees of the incident beam direction, were separated from the incident beam by an electrostatic separator. The device uses electrostatic fields to separate out the transmitted ER from the beam-like particles, allowing in principle only the ER to enter the detection system, which is based on the measurement of the energy and time of flight (TOF) of the ER.

Received 19 January 2010

* Supported by National Natural Science Foundation of China (10575134, 10675169, 10735100) and Major State Basic Research Developing Program (2007CB815003)

1) E-mail: jiahm@ciae.ac.cn

† This device was built in 1986 and reconstructed in 2005.

The beam separation exploits the difference in electrical rigidities $\eta=E/q$ existing in ER and beam-like products (q being the ion charge of the transmitted nuclei). The electrostatic deflector introduced here is similar to the setup in Legnaro [8].

Figure 1 is a schematic layout (top view) of the whole experiment setup (separator + detection system). The separator consists of two pairs of electrodes, of 25 cm in length, 12 cm in width and 0.5 cm in thickness, for each electrical plate, producing two regions of electrostatic field, with independently variable gaps to easily match different experimental conditions and to minimize the possibility of beam scattering from the electrodes. The separator itself is contained in a cylindrical stainless steel tank with a diameter of 30 cm and a length of 85 cm. The plates are at 5° with respect to the beam axis, so that the particles enter the field region at an angel of 85° with respect to the electric field. The applied voltages are such that the ERs leave the field region at 90° to the field, and on the axis of the detection telescope.

The two high voltage power supplies can produce up to ±40 kV. The ER was identified by an E-TOF detector system consisting of a microchannel plate (MCP) detector followed by a silicon surface barrier (SSB) detector. A two-dimensional spectrum of the reaction products was used to cleanly separate the evaporation residues from the beam-like products.

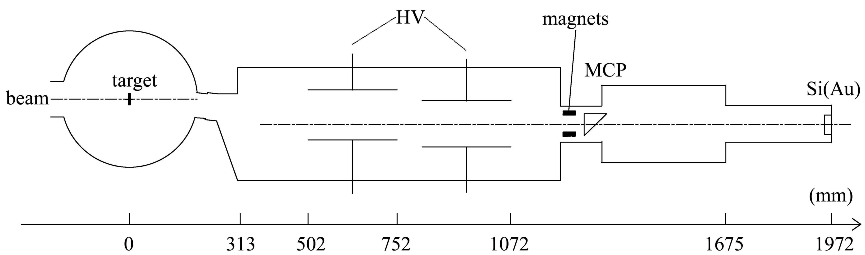

Fig. 1. The layout of the electrostatic deflector and the MCP+Si detection system.

The particles coming from the target are selected before entering the fields by an entrance collimator of 3 mm, corresponding to ±0.57°. A carbon foil, 10 μg/cm^2 in thickness, attached to the collimator to reset the atomic charge state distribution after the fused nuclei have become evaporation residues by the emission of several light particles on the ion path. The electric field strength of the deflectors was selected to maximize the yield of the ER. The diaphragm of the MCP defines the solid angle of the electrostatic deflector approximately as 0.3 msr. In order to reduce the noise of the MCP detector, it was found necessary to place a few small permanent magnets behind the exit collimator of the chamber and in front of the start detector to be against secondary electrons.

The whole apparatus, including the separator and the telescope detectors, is connected to the target chamber by metallic bellows and can be rotated in the horizontal plane from −4° to +12° with respect to the beam, allowing the measurement of ER angular distributions in that range.

3 Experimental test

The experiment was performed at the HI-13 tandem accelerator of CIAE, Beijing. The transmission efficiencies of the ER through the electrostatic deflector were determined empirically by the elastic scattering of the nuclei of vicinal atomic charge, mass and kinetic energy. To perform this, we measured the Rutherford scattering of 29 MeV ^{127}I on the ^{90}Zr target at 10°. The transmission probability was defined as the ratio of the number of particles detected at the SSB detector to that initially passing the entrance collimator. The applied voltages to deflect the reaction products are consistent with the calibrations including the fringe effect of the electrical plates with Shima's charge state distribution formula [10]. In the experiment, the two pairs of electrical plates applied the same voltages with the same electrode distance of 4 cm to facilitate the calculation. In Fig. 2, the transmission efficiency of ^{127}I is plotted versus the applied voltage. As can be seen, the transmission efficiency of the scattered particles is less sensitive to the electric field near the proper value. Considering the transmission of the particles through the electrical harp in the bracket of the MCP detector on the ion path, it is found that the defocusing effect of the deflection voltage reduces the transmission from unity to 0.60±0.06.

A test experiment was performed to test the electrostatic deflector. In the experiment, the collimated ^{32}S 10^+ beam was used to bombard the target with an intensity of 3 pnA. The target was $^{96}ZrO_2$ (86.4%

enriched), 50 μg/cm^2 in thickness and 3 mm in diameter, evaporated onto a 15 μg/cm^2 carbon backing. The scattering chamber contains four silicon detectors at θ=25° symmetrically around the beam in the forward direction to monitor the beam and normalize the fusion cross sections.

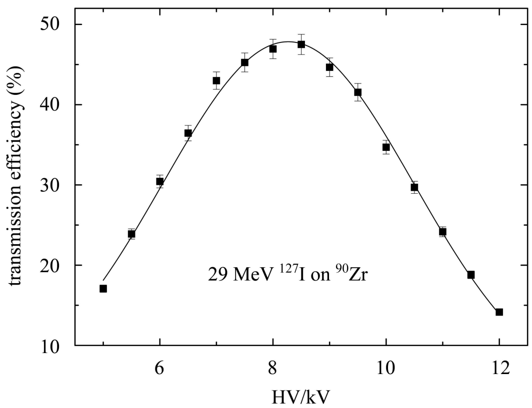

Fig. 2. 29 MeV ^{127}I transmission efficiency as a function of the deflection voltage.

The separated residues were identified in an E-TOF detector telescope, which consisted of a MCP and a SSB with a 60 cm flight path. The combined E and TOF information enabled a clean separation of the evaporation residues from the beam-like particles. The resolution of TOF (the start signal is provided by a ϕ50 SSB on an overbias state and the stop signal is provided by a MCP detector) is about 2 ns, which is suitable to research the topic. As can be seen in Fig. 3, the yields of ER can be obtained, essentially free of background, from the time of flight versus energy spectrum, which shows well separated islands of events. The lower corresponds to the ER from ^{32}S+^{96}Zr reaction, while the stronger consists of the beam-like particles.

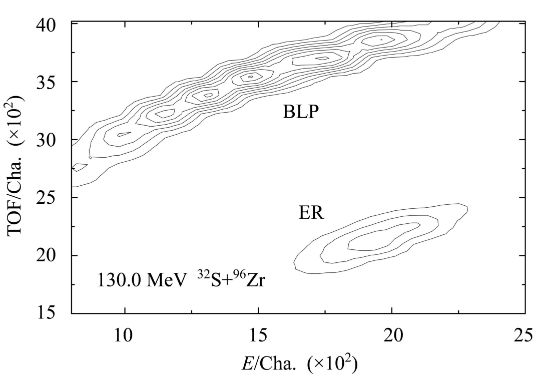

Fig. 3. Two-dimensional plot of time of flight vs energy for the ^{32}S+^{96}Zr reaction at 130.0 MeV and at 2°, following beam separation. Two groups of particles are indicated.

ER angular distributions were measured in the range −4° to 10° with a step of 1° at three beam energies (130.0, 116.4 and 108.3 MeV) and shown in Fig. 4. The angular distributions are symmetric about 0°. Double Gaussian function was used to fit the data, which associated qualitatively the wider Gaussian with the emission of α particles from the recoiling composite system whereas the narrower one results from the neutron and proton evaporation, then integrated to obtain the total fusion cross sections. The shapes do not change appreciably with the beam energy. These combined angular distributions and the double Gaussian fits were used to obtain the fusion cross sections.

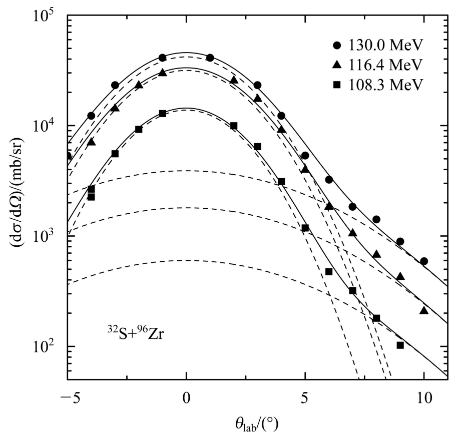

Fig. 4. The angular distributions of fusion evaporation residues of ^{32}S+^{96}Zr at three beam energies. The dashed lines are the two Gaussian functions used to obtain the total cross sections.

For each energy, the number of evaporation residue events was normalized to the Rutherford scattering detected by the monitor detectors. The absolute cross section normalization relies on the knowledge of the relevant geometric solid angle and of the transmission efficiency of the electrostatic deflector. Since fission of the compound nucleus can be neglected for both systems, the measured evaporation residue cross sections were taken as fusion cross section σ. The fusion cross section of ^{32}S+^{96}Zr, at 130 MeV well above the Coulomb barrier, can be calculated with classical transmission probability for a one-dimensional barrier formula. The integrated fusion cross section from the measured angular distribution is 625 mb. Including the transmission efficiency uncertainty, additional systematic errors come from the geometrical solid angle uncertainties and the angular distribution integration measurements. Altogether, these contributions sum up to an estimated ±15%. The experimental result is consistent with the calculation result 601 mb. This result confirms the reliability of the setup.

In the future, the electrostatic deflector will be used to research the fusion reactions primarily near the Coulomb barrier, especially the effects of positive Q-value neutron transfer and breakup of the weakly bound nuclei (^{6,7}Li, ^{9}Be) on the fusion reactions at the sub-barrier energy region.

4 Summary

An electrostatic deflector has been installed and tested by measuring the fusion cross sections of the ^{32}S+^{96}Zr system at three beam energies. The fusion evaporation residues were separated from the beam-like particles by this device. By integrating the ER angular distributions, one obtains the ER cross sections. The experimental result is in good agreement with the theoretical value well above the Coulomb barrier. This device is reliable and will mainly be used to research the effect of the weakly bound projectiles and neutron-rich effect of the participants in the fusion reactions around the Coulomb barrier energies.

References

1 Timmers H, Ackermann D, Beghini S et al. Nucl. Phys. A, 1998, **633**: 421

2 Hinde D J, Dasgupta M, Fulton B R et al. Phys. Rev. Lett., 2002, **89**: 272701

3 Stelson P H. Phys. Lett. B, 1988, **25**: 25

4 Stefanini A M, Scarlassara F, Beghini S et al. Phys. Rev. C, 2006, **73**: 034606

5 LIANG J F, Shapira D, Gross C J et al. Phys. Rev. Lett., 2003, **91**: 152701

6 JIANG C L, Esbensen H, Rehm K E et al. Phys. Rev. Lett., 2002, **89**: 052701

7 Freeman W S, Ernst H, Geesaman D F et al. Phys. Rev. Lett., 1983, **50**: 1563

8 Beghini S, Signorini C, Lunardi S et al. Nucl. Instrum. Methods A, 1985, **239**: 585

9 Schicker R, Alamanos N, Braun-Munzinger P et al. Nucl. Instrum. Methods A, 1988, **269**: 585

10 Shima K, Kuno N, Yamanouchi M et al. At. Data and Nucl. Data Table, 1992, **51**: 173